

Zero-frequency anomaly in quasiclassical ac transport: Memory effects in a two-dimensional metal with a long-range random potential or random magnetic field

J. Wilke

Institut für Theorie der Kondensierten Materie, Universität Karlsruhe, 76128 Karlsruhe, Germany

A. D. Mirlin*

*Institut für Theorie der Kondensierten Materie, Universität Karlsruhe, 76128 Karlsruhe, Germany
and Institut für Nanotechnologie, Forschungszentrum Karlsruhe, 76021 Karlsruhe, Germany*

D. G. Polyakov[†]

Institut für Nanotechnologie, Forschungszentrum Karlsruhe, 76021 Karlsruhe, Germany

F. Evers

Institut für Theorie der Kondensierten Materie, Universität Karlsruhe, 76128 Karlsruhe, Germany

P. Wölfle

*Institut für Theorie der Kondensierten Materie, Universität Karlsruhe, 76128 Karlsruhe, Germany
and Institut für Nanotechnologie, Forschungszentrum Karlsruhe, 76021 Karlsruhe, Germany*

(Received 11 November 1999)

We study the low-frequency behavior of the ac conductivity $\sigma(\omega)$ of a two-dimensional fermion gas subject to a smooth random potential (RP) or random magnetic field (RMF). We find a nonanalytic $\propto |\omega|$ correction to $\text{Re } \sigma$, which corresponds to a $1/t^2$ long-time tail in the velocity correlation function. This contribution is induced by return processes neglected in Boltzmann transport theory. The prefactor of this $|\omega|$ term is positive and proportional to $(d/l)^2$ for the RP, while it is of opposite sign and proportional to d/l in the weak RMF case, where l is the mean free path and d the disorder correlation length. This nonanalytic correction also exists in the strong RMF regime, when the transport is of a percolating nature. The analytical results are supported and complemented by numerical simulations.

I. INTRODUCTION

Within the conventional approach based on the Boltzmann equation, the ac conductivity of a two-dimensional electron gas (2DEG) is described by the Drude formulas

$$\sigma_D(\omega) = \frac{\sigma_0}{1 - i\omega\tau}, \quad (1)$$

$$\sigma_0 = e^2 \nu D, \quad D = \frac{v_F^2 \tau}{2}, \quad (2)$$

where τ is the transport time, ν the density of states at the Fermi level, v_F the Fermi velocity, and D the diffusion constant. Equation (1) corresponds to an exponential falloff of the velocity correlation function in the time representation,

$$\langle \mathbf{v}(t) \mathbf{v}(0) \rangle = v_F^2 e^{-t/\tau}, \quad t > 0. \quad (3)$$

This exponential behavior of $\langle \mathbf{v}(t) \mathbf{v}(0) \rangle$ reflects the Markovian character of the Boltzmann equation description, and leads to the analytical behavior of $\sigma_D(\omega)$ at $\omega \rightarrow 0$. It has been known for almost three decades, however, that these features result from approximations made in the derivation of the Boltzmann equation, and are not generally shared by the exact solution of the problem. More specifically, it was shown¹ (see also Ref. 2 for a review and Ref. 3 for numerical simulations) that in the Lorentz gas model, where a particle

is scattered by randomly located hard discs of radius a and density n_s , there exists a ‘‘long-time tail’’ of the velocity correlation function, which has the following form in two dimensions in the limit $n_s a^2 \ll 1$:

$$\langle \mathbf{v}(t) \mathbf{v}(0) \rangle = -\frac{1}{4\pi n_s t^2}. \quad (4)$$

This leads to a correction to the Drude conductivity, which is nonanalytic at $\omega \rightarrow 0$,

$$\Delta \text{Re } \sigma(\omega) = \sigma_0 \frac{1}{8n_s l^2} |\omega| \tau = \sigma_0 \frac{a}{3l} |\omega| \tau, \quad |\omega| \tau \ll 1, \quad (5)$$

where $l = v_F \tau$ is the mean free path, and we substituted $l = 3/8n_s a$, an expression valid for the hard disc model. We will refer to this type of behavior of $\sigma(\omega)$ as a ‘‘classical zero-frequency anomaly.’’ The long-time tail [which is of the form $t^{-(d+2)/2}$ in d dimensions] can be traced back to processes of return of a particle to a region of extension $\sim l$ around the starting point after moving diffusively during the time $t \gg \tau$.⁴ These return processes give rise to non-Markovian kinetics, and are neglected in the Boltzmann equation.

After the discovery of weak localization the research interest has shifted from the above (purely classical) effects to

quantum corrections to the conductivity. For a noninteracting 2D Fermi gas the quantum (weak localization) correction is given by⁵

$$\Delta\sigma_{\text{wl}}(\omega) = \sigma_0 \frac{1}{\pi k_F l} \ln|\omega\tau|, \quad (6)$$

where k_F is the Fermi wave vector. The weak-localization correction is of special interest, in particular, since it is divergent at zero frequency, indicating a crossover to strong localization. However, for weak disorder, $k_F l \gg 1$, the strong localization is of purely academic interest, for its observation would require an exponentially small frequency and temperature and exponentially large system size.

In recent years, there has been a revival of interest in semiclassical transport properties of 2DEG's. This is motivated by the experimental and technological importance of high-mobility semiconductor heterostructures, where impurities are located in a layer separated by a large spacer $d \sim 100$ nm from the 2DEG plane. The (screened) random potential (RP) $V(\mathbf{r})$ produced in the 2DEG plane by the statistically distributed charged impurities (density n_i) is characterized by the correlation function $W_V(\mathbf{r}-\mathbf{r}') = \langle V(\mathbf{r})V(\mathbf{r}') \rangle$, which has in momentum space the form

$$\tilde{W}_V(q) = (\pi\hbar^2/m)^2 n_i e^{-2qd}, \quad (7)$$

where m is the particle mass. For $k_F d \gg 1$ (which is well satisfied for the high-mobility samples), the potential varies smoothly in space, and can be treated in semiclassical terms. Such a random potential is different from the Lorentz gas model in an essential way. It is weak everywhere, and shows close-to-Gaussian fluctuations (since at $n_i d^2 \gg 1$ potentials produced by adjacent scatterers strongly overlap), whereas in the Lorentz gas the potential is zero outside scatterers and infinite inside scatterers. Therefore, the Lorentz gas results cannot be directly applied to the 2DEG, and the problem has to be reconsidered for a realistic model of the random potential.

Transport in a smoothly varying random magnetic field (RMF) is also of major interest. One of the main motivations for this comes from the relevance of this problem to the composite-fermion description of a 2DEG in a strong magnetic field in the vicinity of half-filling of the lowest Landau level ($\nu=1/2$).⁶ Exactly at $\nu=1/2$ the composite fermions move in an effective magnetic field $B(\mathbf{r})$ with zero average and impurity-induced spatial fluctuations characterized by a correlation function $W_B(\mathbf{r}-\mathbf{r}') = \langle B(\mathbf{r})B(\mathbf{r}') \rangle$ of the form

$$\tilde{W}_B(q) = (2hc/e)^2 n_i e^{-2qd}. \quad (8)$$

A real long-range RMF can also be realized in semiconductor heterostructures by attaching superconducting^{7,8} or ferromagnetic⁹⁻¹¹ overlayers or by pre patterning of the sample (randomly curving the 2DEG layer).¹² The strength of a RMF can be conveniently characterized^{13,14} by a dimensionless parameter $\alpha = d/R_c^0$, where $R_c^0 = v_F m c / e B_0$ is the cyclotron radius in a typical field $B_0 = \sqrt{\langle B^2 \rangle}$ (the magnitude of the RMF fluctuations). Within the composite-fermion theory of Ref. 6 this parameter is found to be equal to $1/\sqrt{2}$, if the density of ionized impurities n_i is assumed to be equal to the electron density n and if correlations between the im-

purity positions are neglected. Experimental data for the magnetoresistivity around $\nu=1/2$ are well described by the theory,¹⁵ with somewhat smaller $\alpha \approx 0.2-0.35$ (the deviation can be presumably attributed to the Coulomb correlations in positions of impurities and other possible features related to technological details of the sample preparation, as well as to approximations in the composite-fermion theory). We will concentrate in the main part of this paper on the weak RMF case, $\alpha \ll 1$, when the transport is of conventional diffusive nature. The long-time tail in the case $\alpha \gg 1$ (snake-state transport) will be discussed in Sec. III C.

The following historical remark is in order here. After the initial paper¹ by Ernst and Weyland on the Lorentz gas model, the $t^{-(d+2)/2}$ tail in the velocity correlation function of a gas of particles scattered by static impurities was discussed in a number of publications; see, in particular, Refs. 16 and 17. However, since there appear to be neither a clear derivation nor explicit results for the long-time tail in a smooth RP in the literature, we decided to present this material in a self-contained form (Secs. II A and III A). In fact, our Eq. (16) can be obtained from the mode-coupling formalism of Ref. 18; however, the authors of that paper concentrated on the critical regime of the metal-insulator transition, and did not consider the ac conductivity in the conducting phase explicitly. As to the RMF problem, which constitutes the main focus of the present paper, we are not aware of any treatment of the classical nonanalytic correction to the ac conductivity in the literature.

For later use, here we recall the transport scattering rate entering the Drude formulas (1) and (2), which, in the case of weak long-range disorder, is found to be¹⁹

$$\frac{1}{\tau} = \frac{1}{2\pi m^2 v_F^3} \int_0^\infty dq q^2 \tilde{W}_V(q) \quad (\text{RP}), \quad (9)$$

$$\frac{1}{\tau} = \left(\frac{e}{mc}\right)^2 \frac{1}{2\pi v_F} \int_0^\infty dq \tilde{W}_B(q) \quad (\text{RMF}). \quad (10)$$

Let us note that the Drude result is valid in the quantum regime as well as in the classical limit. This is not, however, the case for corrections to the Drude result and we will therefore consider both a quantum theoretical treatment and a purely classical description, for different parameter ranges.

We recall that the classical description of a quantum particle moving in a RP or RMF characterized by a single spatial scale is a good approximation if two conditions are satisfied: (i) the quantum-mechanical wavelength of the particle should be less than the characteristic length d of the disorder, i.e., $k_F d \gg 1$; (ii) the particle should move incoherently, i.e., the length over which it is scattered out of its initial quantum state should be less than d : $v_F \tau_s \ll d$, where τ_s is the single-particle lifetime. The latter condition requires the random field to be sufficiently strong. We will not address the regime $k_F d \gg 1$ and $v_F \tau_s \gg d$ in this paper. Our choice of models of disorder is motivated by actual physical realizations and by considerations of calculational feasibility. We will consider either a long-range RP or RMF governed by Gaussian statistics. In the quantum-mechanical calculation, we will assume the transport scattering rate to be dominated by a white-noise RP.

As discussed above in the context of the Lorentz gas, the fact that a particle may revisit a given region of a RP/RMF after large time t gives rise to a zero-frequency anomaly of the conductivity. Due to this effect, the velocity correlation function acquires a power-law behavior $\propto t^{-2}$ at long times, leading to $\text{Re}\sigma(\omega) \propto |\omega|$. The strength of this anomaly depends on the probability of return into the region over which the RP or RMF is correlated, and may thus be expected to be proportional to a power of d/l (the power depends on the mechanism of scattering). For a short-range potential, $k_F d \lesssim 1$, the role of the effective correlation length is played by the Fermi wavelength. It is worth stressing that the quantum corrections to the conductivity are governed by another parameter, namely, $1/k_F l$. It follows that the magnitude of the classical zero-frequency anomaly for the case of smooth disorder $k_F d \gg 1$, which is the limit considered here, may be much larger than the quantum corrections in a broad frequency range. For composite fermions, the parameter $k_F d$ is as large as 15. The quantum corrections, being proportional to $\ln\omega$ (at zero temperature), then become important only in the limit of very small (in fact, exponentially small) frequency. Moreover, as we discuss in Sec. IV, inelastic scattering at finite temperature destroys the quantum corrections but does not affect the classical correction. Hence the conditions for the observation of the classical anomaly become still more favorable at finite T . We now turn to a calculation of the low-frequency correction to the Drude law induced by the return processes.

II. RETURN PROCESSES IN THE QUANTUM-MECHANICAL DIAGRAM TECHNIQUE

We begin by considering the case in which the leading contribution to the transport scattering rate is given by a white-noise RP, while an additional weak long-range RP or RMF induces correlations determining the long-time tail. In this situation, a quantum-mechanical treatment of the problem is appropriate. Apart from the theoretical convenience, such a model with two types of disorder is also of experimental relevance. Indeed, in essentially all realizations of *real* RMF (as opposed to the fictitious RMF in the composite-fermion model) the transport scattering rate is dominated by a random potential with a relatively short correlation length (much shorter than that of the RMF).

A white-noise RP is characterized by the correlation function $\tilde{W}(q) = (2\pi\nu\tau_w)^{-1}$, where $1/\tau_w$ is the corresponding scattering rate (here we put $\hbar = 1$). We keep the notation $1/\tau$ for the scattering rate related to a long-range RP or RMF: $1/\tau \ll 1/\tau_w$. The diffusion process is described by a sum of the ladder diagrams (a diffuson),

$$\Gamma(\mathbf{q}, \omega) = \frac{1}{2\pi\nu\tau_w^2} \frac{1}{Dq^2 - i\omega}, \quad (11)$$

where $D = v_F^2 \tau_w / 2$.

A. Long-range random potential

The contribution to the conductivity induced by return processes is given by the sum of the diagrams shown in Fig. 1, yielding

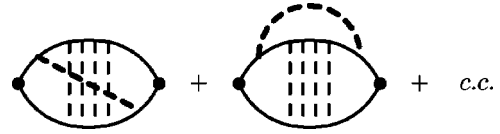


FIG. 1. Contribution to the conductivity due to return processes in the presence of a long-range RP. The thin dashed lines (forming a diffusion) correspond to a white-noise potential, while the thick dashed line describes the long-range RP.

$$\Delta\sigma = \frac{e^2}{2\pi} \int \frac{d^2q}{(2\pi)^2} S_x S_x \tilde{W}_V(q) \Gamma(\mathbf{q}, \omega). \quad (12)$$

Here S_x are the vertex parts which are represented in Fig. 2, and are given by the expression

$$S_x = \int \frac{d^2p}{(2\pi)^2} \frac{p_x}{m} G_{\epsilon_F}^R(\mathbf{p}) G_{\epsilon_F}^A(\mathbf{p}) [G_{\epsilon_F}^R(\mathbf{p}-\mathbf{q}) + G_{\epsilon_F}^A(\mathbf{p}+\mathbf{q})], \quad (13)$$

where $G_{\epsilon_F}^R(\mathbf{p})$ and $G_{\epsilon_F}^A(\mathbf{p})$ are the retarded and advanced Green's functions at the Fermi energy ϵ_F .

The behavior of the correction $\Delta\sigma(\omega)$ at low ω is governed by small momenta $q \sim (\omega/D)^{1/2}$ in integral (12). Therefore, we can make a small- q expansion of the vertex part [Eq. (13)]. Expanding the integrand of Eq. (13) up to terms linear in q ,²⁰ we obtain

$$S_x(\mathbf{q}) = -iq_x \tau_w^2. \quad (14)$$

Note that a naive estimate of the linear-in- q term would give $S_x(\mathbf{q}) \sim q_x \epsilon_F \tau_w^3$, but the two diagrams of Fig. 2 cancel each other in this order, and one has to go to the next order in $1/\epsilon_F \tau_w$. Substituting Eqs. (14), (11), and (7) into Eq. (12), approximating the correlation function $\tilde{W}_V(q)$ for small q by its zero- q value, and neglecting the ω -independent part, we find the following ω -dependent contribution to the conductivity:

$$\Delta\sigma(\omega) = \sigma_0 \frac{\tilde{W}_V(0)}{4\epsilon_F^2 l_w^2} \frac{\omega \tau_w}{i\pi} \ln(i\omega \tau_w), \quad |\omega| \tau_w \ll 1. \quad (15)$$

The correction to the real part of the conductivity therefore has the form

$$\Delta \text{Re} \sigma(\omega) = \sigma_0 \frac{\tilde{W}_V(0)}{8\epsilon_F^2 l_w^2} |\omega| \tau_w, \quad |\omega| \tau_w \ll 1. \quad (16)$$

The condition of validity $|\omega| \tau_w \ll 1$ given above corresponds to the case $d \lesssim l_w$. In the opposite regime, $d \gg l_w$, formulas (15) and (16) still hold, but the condition of their validity changes to $|\omega| \ll D/d^2$. The same is valid for all the formulas for the nonanalytic correction that are given below.

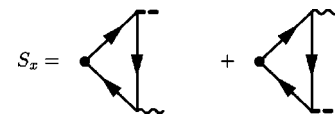


FIG. 2. Vertex parts of the diagrams shown in Fig. 1. The wavy line denotes the diffuson.

We first consider the situation with only the white-noise potential present, so that $\tilde{W}_V(q) = \tilde{W}_V(0)$. In this case, Eq. (16) yields

$$\frac{\Delta \text{Re } \sigma(\omega)}{\sigma_0} = \frac{1}{2(k_F l_w)^3} |\omega| \tau_w. \quad (17)$$

We see that the correction is small as $(k_F l_w)^{-3}$, i.e., much smaller than the weak-localization correction (6), and is therefore of minor interest. This conclusion changes, however, when we return to the problem with the long-range potential (7) present. Equation (16) then gives

$$\frac{\Delta \text{Re } \sigma(\omega)}{\sigma_0} = 4\pi \frac{\tau_w}{\tau} \left(\frac{d}{l_w}\right)^3 |\omega| \tau_w. \quad (18)$$

Now the correction does not contain the quantum small parameter $(k_F l_w)^{-1}$, which is replaced by the classical quantity d/l_w . This prompts the expectation that the $|\omega|$ anomaly in $\sigma(\omega)$ should be essentially a classical phenomenon. We will demonstrate this explicitly in Sec. III by calculating $\Delta \text{Re } \sigma(\omega)$ in the classical limit, where a long-range RP constitutes the only type of disorder in the system. Note that the classical limit requires two conditions to be met: $k_F d \gg 1$ for all relevant types of scatterers, and also $\tilde{W}_V(0) \gg (\hbar v_F)^2$ (the latter condition means smallness of the diffraction smearing of a typical scattering angle; otherwise, it can be rewritten as $v_F \tau_s \ll d$, where τ_s is the single-particle lifetime); whereas Eq. (18) is obtained in the perturbative (Born) limit $\tilde{W}_V(0) \ll (\hbar v_F)^2$ under the condition that the diffusion is due to short-range scatterers. It is also worth mentioning here that, in view of $\tau \gg \tau_w$ and $v_F \tau \gg d$, correction (18) is always small, $\Delta \text{Re } \sigma(\omega)/\sigma_0 \ll 1$, in the range of its validity [specified below Eq. (16)].

B. Long-range random magnetic field

We now consider the same problem but with the long-range RP replaced by a long-range RMF. Similarly to Eq. (12), we have a return-induced correction to the conductivity

$$\Delta \sigma = \frac{e^2}{2\pi} \sum_{\alpha\beta} \int \frac{d^2 q}{(2\pi)^2} (S_{x\alpha}^{(1)} + S_{x\alpha}^{(2)}) (S_{x\beta}^{(1)} + S_{x\beta}^{(2)}) \times \langle A^\alpha(\mathbf{q}) A^\beta(-\mathbf{q}) \rangle \Gamma(\mathbf{q}, \omega), \quad (19)$$

where

$$\langle A^\alpha(\mathbf{q}) A^\beta(-\mathbf{q}) \rangle = \frac{\tilde{W}_B(q)}{q^2} (\delta_{\alpha\beta} - \hat{q}_\alpha \hat{q}_\beta), \quad \hat{q}_\alpha = \frac{q_\alpha}{|\mathbf{q}|} \quad (20)$$

is the vector potential correlation function. The vertex part $S_{x\alpha}^{(1)} + S_{x\alpha}^{(2)}$ is now given by the sum of the three diagrams shown in Fig. 3.

Evaluating the vertex part at small q , we find that the diagrams $S_{x\alpha}^{(1)}$ and $S_{x\alpha}^{(2)}$ cancel each other in the order q^0 , and the result is of the order of q^2 :

$$S_{x\alpha}^{(1)} + S_{x\alpha}^{(2)} = -\frac{e}{mc} q^2 \epsilon_F \tau_w^3 \delta_{x\alpha}. \quad (21)$$

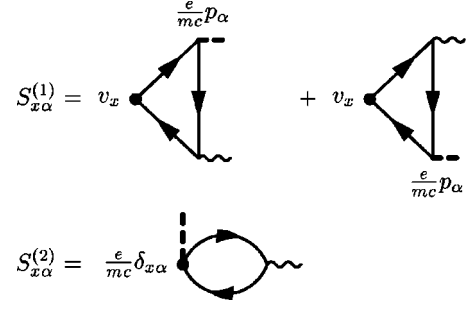


FIG. 3. Vertex parts of diagrams in a random magnetic field.

Substituting this expression into Eq. (19) and neglecting an ω -independent part, we find

$$\frac{\Delta \text{Re } \sigma(\omega)}{\sigma_0} = -\left(\frac{e}{mc}\right)^2 \frac{\tilde{W}_B(0)}{8v_F^2} |\omega| \tau_w, \quad |\omega| \tau_w \ll 1. \quad (22)$$

Using the explicit form of the correlation function (8), we obtain

$$\frac{\Delta \text{Re } \sigma(\omega)}{\sigma_0} = -\frac{\pi d}{2l} |\omega| \tau_w, \quad (23)$$

where $l = v_F \tau$ is the mean free path characterizing the RMF. We see that the nonanalytic conductivity correction (and correspondingly the long-time tail of the velocity correlation function) has the opposite sign as compared to the RP case [Eq. (18)]. This is a general feature of the corrections induced by a weak long-range RMF, as will be confirmed in Sec. III B by a classical calculation for the case when such a RMF constitutes the only source of disorder.

III. PURELY LONG-RANGE DISORDER: CLASSICAL CALCULATION OF THE LONG-TIME TAILS

Having understood the nature of the $|\omega|$ anomaly at the level of the quantum-mechanical diagram technique in the particular limit where the transport scattering rate is dominated by a white-noise potential, we turn to the case of purely long-range disorder (RP or RMF). In this situation, the quantum-mechanical calculation is complicated, and a classical evaluation of the nonanalytic correction is more appropriate; this will also allow us to demonstrate explicitly that the correction is of classical origin. We will employ a formalism similar to the one used in Ref. 21 for a calculation of the magnetoresistivity. At the quasiclassical level, the fermion gas is characterized by a distribution function $f(t, \mathbf{r}, \phi)$, where ϕ is the polar angle of the velocity. The equilibrium distribution function is $f_0 = \theta(\epsilon_F - \epsilon)$, where θ is the step function. The deviation $\delta f(t, \mathbf{r}, \phi)$, from the equilibrium induced by an (infinitesimally small) external electric field $\mathbf{E} e^{-i\omega t}$, has the form $\delta f(t, \mathbf{r}, \phi) = e E v_F (\partial f_0 / \partial \epsilon) e^{-i\omega t} g(\omega, \mathbf{r}, \phi)$, with $g(\omega, \mathbf{r}, \phi)$ obeying the Liouville equation

$$(L_0 + \delta L) g(\omega, \mathbf{r}, \phi) = \cos(\phi - \phi_E), \quad (24)$$

$$L_0 = -i\omega + v_F \mathbf{n} \nabla. \quad (25)$$

Here ϕ_E is the polar angle of the electric field and $\mathbf{n} = (\cos \phi, \sin \phi)$ the unit vector determining the velocity di-

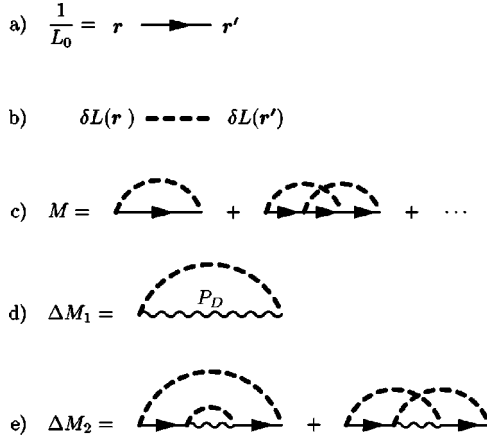


FIG. 4. Classical diagram technique: (a) Free propagator. (b) Disorder correlation function. (c) Diagrammatic expansion for the memory function M . (d) First-order diagram for the memory function representing a return process; the wavy line corresponds to the diffusion propagator P_D [Eq. (31)]. (e) Second-order diagrams describing return processes, which give the leading contribution to the return-induced correction to M in the random-potential case.

rection. The term L_0 in the Liouville operator corresponds to the free motion, while δL describes the disorder (RP or RMF). The current density is given by $\mathbf{j} = -e \int [d^2 p / (2\pi\hbar)^2] \mathbf{v} \delta f$, yielding the longitudinal conductivity

$$\sigma(\omega) = e^2 \nu v_F^2 \int \frac{d\phi}{2\pi} \left\langle \cos \phi \frac{1}{L_0 + \delta L} \cos \phi \right\rangle. \quad (26)$$

Expanding Eq. (26) in δL , averaging over the RP or RMF (which is implicit in δL), and resumming the series, we obtain the ac conductivity in the form

$$\sigma(\omega) = \frac{\sigma_0 / \tau}{-i\omega + M}. \quad (27)$$

Here M is the self-energy (the so-called memory function), which can be conveniently represented within a classical diagrammatic technique (similar to the one used in Ref. 17) (Fig. 4). To leading order, M is given by the first diagram of Fig. 4(c),

$$M_0 = -2 \int \frac{d\phi}{2\pi} \cos \phi \left\langle \delta L \frac{1}{L_0} \delta L \right\rangle \cos \phi, \quad (28)$$

reproducing results (9) and (10) for the transport scattering rate (see below) and, correspondingly, the Drude formula (1). Corrections to the memory function $M(\omega)$, which correspond to the return processes, are evaluated in Secs. III A and III B for the cases of RP and RMF, respectively.

A. Long-range random potential

The fluctuating contribution to the Liouville operator due to the RP is found to be

$$\delta L_V = \delta v(\mathbf{r}) \mathbf{n} \nabla + [\nabla \delta v(\mathbf{r})] \mathbf{n}_\perp \frac{\partial}{\partial \phi}, \quad (29)$$

where $\mathbf{n}_\perp = \hat{\mathbf{z}} \times \mathbf{n} = (-\sin \phi, \cos \phi)$, and $\delta v(\mathbf{r}) = v(\mathbf{r}) - v_F$ is the deviation of the local velocity $v(\mathbf{r}) = \{(2/m)[\epsilon_F - V(\mathbf{r})]\}^{1/2}$ from its average value v_F . The leading-order contribution (28) to the memory function reads

$$M_0 = -\frac{2i}{p_F^2} \int \frac{d\phi}{2\pi} \frac{d^2 q}{(2\pi)^2} \sin \phi \sin(\phi - \phi_q) \times \frac{q^2 \tilde{W}_V(q)}{v_F q \cos(\phi - \phi_q) - \omega - i0} \sin \phi \sin(\phi - \phi_q), \quad (30)$$

reproducing the transport scattering rate defined by Eq. (9): $M_0 = 1/\tau$. The first-order diagram describing the return process is represented in Fig. 4(d). The corresponding expression is obtained by replacing the free propagator $1/L_0$ in Eq. (30) by the diffusion propagator

$$P_D(\mathbf{q}, \phi, \phi') = \frac{\gamma(\mathbf{q}, \phi) \gamma(\mathbf{q}, \phi')}{Dq^2 - i\omega}, \quad (31)$$

$$\gamma(\mathbf{q}, \phi) \approx 1 - iql \cos(\phi - \phi_q), \quad ql \ll 1.$$

The replacement yields the return-induced first-order correction to the memory function:

$$\Delta M_1 = \frac{2}{p_F^2} \int \frac{d\phi}{2\pi} \frac{d\phi'}{2\pi} \frac{d^2 q}{(2\pi)^2} \sin \phi \sin(\phi - \phi_q) \times q^2 \tilde{W}_V(q) P_D(\mathbf{q}, \phi, \phi') \sin \phi' \sin(\phi' - \phi_q). \quad (32)$$

Evaluating the ω -dependent part of Eq. (32) at $\omega\tau \ll 1$, and approximating (as in the quantum-mechanical calculation) $\tilde{W}_V(q)$ by its value at $q=0$, we find

$$\frac{\Delta M_1(\omega)}{M_0} = -\frac{\tilde{W}_V(0)}{16\epsilon_F^2 l^2} \frac{\omega\tau}{i\pi} \ln(i\omega\tau), \quad (33)$$

which gives

$$\frac{\Delta \text{Re } M_1(\omega)}{M_0} = -\pi \left(\frac{d}{l}\right)^3 |\omega| \tau \quad (34)$$

for the specific form [Eq. (7)] of the correlator \tilde{W}_V .

Now let us show that, in actual fact, the leading contribution to the non-Markovian correction to $\text{Re } M(\omega)$ comes from second-order processes described by the two diagrams in Fig. 4(e), whereas that given by Eq. (33) can be neglected in the first approximation. Specifically, the second-order term $\Delta \text{Re } M_2 / M_0 \sim (d/l)^2 |\omega| \tau$ scales with a smaller, as compared to ΔM_1 , power of the parameter $d/l \ll 1$, despite having one more impurity line. This, at first glance, counter-intuitive feature is related to the anomalous smallness of ΔM_1 in the otherwise ‘‘regular’’ expansion in powers of d/l (third- and higher-order terms in ΔM can be shown to be negligible compared to ΔM_2). We first explain this feature by using the following power-counting argument. The $|\omega|$ anomaly in ΔM comes from the integration over small q of

the form $\int d^2q q^2/(Dq^2 - i\omega)$, where the numerator of the integrand tends to zero as q^2 at $q \rightarrow 0$. In Eq. (32), the factor of q^2 is related to the vanishing of the correlator

$$\int d^2r \exp(-i\mathbf{q}\mathbf{r}) \langle \nabla \delta v(0) \nabla \delta v(\mathbf{r}) \rangle \propto q^2 \tilde{W}_V(q)$$

in the limit $q \rightarrow 0$, since the correlator carries the small momentum q , the same as the diffuson, according to Fig. 4(d). On the other hand, in second order in \tilde{W}_V , the large momenta flowing through impurity lines are ‘‘disentangled’’ from the small momentum q carried by the diffuson. The leading q^2 term now comes from the $O(ql)$ corrections to the diffusion propagator given by the factors $\gamma(\mathbf{q}, \phi)$ in Eq. (31). Let us count powers of l : two factors $\gamma(\mathbf{q}, \phi)$ yield $q^2 l^2$, whereas one loses only l^{-1} when going to second order, which explains the total gain of one power of l/d as compared to Eq. (34).

The expression for ΔM_2 at $\omega \rightarrow 0$ obtained from the sum of the two diagrams in Fig. 4(e) reads [we neglect the dependence on q everywhere but in $P_D(\mathbf{q}, \phi, \phi')$]

$$\begin{aligned} \Delta M_2 = & \frac{4i}{p_F^4} \int \frac{d\phi}{2\pi} \frac{d\phi'}{2\pi} \frac{d^2q}{(2\pi)^2} \frac{d^2k}{(2\pi)^2} k^4 \tilde{W}_V^2(k) \\ & \times \cos \phi A(\mathbf{k}, \phi) P_D(\mathbf{q}, \phi, \phi') \text{Im} A(\mathbf{k}, \phi') \cos \phi', \end{aligned} \quad (35)$$

where

$$A(\mathbf{k}, \phi) = \frac{\partial}{\partial \phi} \frac{\sin^2(\phi - \phi_k)}{v_F k \cos(\phi - \phi_k) - i0} \frac{\partial}{\partial \phi}. \quad (36)$$

We thus obtain

$$\frac{\Delta \text{Re} M_2(\omega)}{M_0} = - \frac{|\omega| \tau}{32\epsilon_F^4} \int \frac{d^2k}{(2\pi)^2} k^2 \tilde{W}_V^2(k). \quad (37)$$

Since

$$\frac{\Delta \text{Re} \sigma(\omega)}{\sigma_0} \simeq - \frac{\Delta \text{Re} M(\omega)}{M_0} \equiv \frac{\Delta \text{Re} \rho(\omega)}{\rho_0}, \quad (38)$$

where $\rho(\omega) = \sigma^{-1}(\omega)$ is the ac resistivity, we finally obtain, using Eq. (7) for \tilde{W}_V ,

$$\frac{\Delta \text{Re} \sigma(\omega)}{\sigma_0} = \frac{3\pi}{8} \left(\frac{d}{l} \right)^2 |\omega| \tau, \quad |\omega| \tau \ll 1. \quad (39)$$

The prefactor of the $|\omega|$ correction to $\text{Re} \sigma(\omega)$ is positive, as in the quantum-mechanical result [Eq. (18)] and in the Lorentz gas formula [Eq. (5)]. Note that the correction [Eq. (39)] matches that for the Lorentz gas [Eq. (5)] at $n_s d^2 \sim 1$, as expected—since this condition separates two extremes of strongly non-Gaussian (Lorentz gas) and Gaussian [Eq. (7)] disorder. On the other hand, the crossover between Eqs. (39) and (18) occurs when the two following conditions are fulfilled: $k_F d \sim 1$ and $\tilde{W}_V(0) \sim (\hbar v_F)^2$ [cf. the definition of the classical limit for Gaussian disorder after Eq. (18)].

B. Long-range random magnetic field

The fluctuating contribution to the Liouville operator induced by the RMF has the form

$$\delta L_B = \frac{e}{mc} B(\mathbf{r}) \frac{\partial}{\partial \phi}. \quad (40)$$

The lowest-order contribution (28) to the memory function

$$\begin{aligned} M_0 = & -2i \left(\frac{e}{mc} \right)^2 \int \frac{d\phi}{2\pi} \frac{d^2q}{(2\pi)^2} \\ & \times \sin \phi \frac{\tilde{W}_B(q)}{v_F q \cos(\phi - \phi_q) - \omega - i0} \sin \phi \end{aligned} \quad (41)$$

again reproduces the corresponding transport scattering rate [Eq. (10)], $M_0 = 1/\tau$. The first-order correction due to return processes [Fig. 4(d)] reads

$$\begin{aligned} \Delta M_1 = & 2 \left(\frac{e}{mc} \right)^2 \int \frac{d\phi}{2\pi} \frac{d\phi'}{2\pi} \frac{d^2q}{(2\pi)^2} \sin \phi \tilde{W}_B(q) \\ & \times P_D(\mathbf{q}, \phi, \phi') \sin \phi', \end{aligned} \quad (42)$$

where the factors $\gamma(\mathbf{q}, \phi)$ should be included in $P_D(\mathbf{q}, \phi, \phi')$, which gives

$$\frac{\Delta \text{Re} \sigma(\omega)}{\sigma_0} = - \frac{\Delta \text{Re} M(\omega)}{M_0} = - \left(\frac{e}{mc} \right)^2 \frac{\tilde{W}_B(0)}{8v_F^2} |\omega| \tau. \quad (43)$$

Note that, in contrast to the case of RP, the leading contribution to the return-induced correction ΔM in the RMF comes from the first-order processes. This is because the RMF scattering operator δL_B (in contrast to its RP counterpart δL_V) does not involve spatial gradients. Using the RMF correlation function [Eq. (8)], we finally obtain

$$\frac{\Delta \text{Re} \sigma(\omega)}{\sigma_0} = - \frac{\pi d}{2 l} |\omega| \tau = - \pi \alpha^2 |\omega| \tau, \quad |\omega| \tau \leq 1. \quad (44)$$

We have found, therefore, in agreement with the quantum-mechanical result [Eq. (23)], a negative sign of the $|\omega|$ contribution to the conductivity. Analyzing the calculation, one can trace the difference in sign [as compared to the Lorentz gas result (5) and the RP results (18) and (39)] back to the fact that the RMF scattering operator (40) is odd with respect to time reversal.

To check the above analytic findings, we have performed numerical simulations of the classical motion of a particle in a RMF. The results obtained for the memory function²² at $\alpha = 0.5$ are shown in Fig. 5. We find a positive $|\omega|$ correction to the real part of the memory function (or, equivalently, resistivity), which corresponds to a negative correction to $\text{Re} \sigma$, in agreement with the theoretical result [Eq. (44)]. The magnitude of the correction is, however, considerably smaller than Eq. (44) would predict. We attribute this discrepancy to the fact that Eq. (44) was derived for $\alpha \ll 1$ and, apparently, the numerical value of the coefficient in this formula cannot be trusted for α as large as 0.5.²³ Unfortunately, at smaller values of $\alpha \leq 0.2$, the effect becomes so weak that

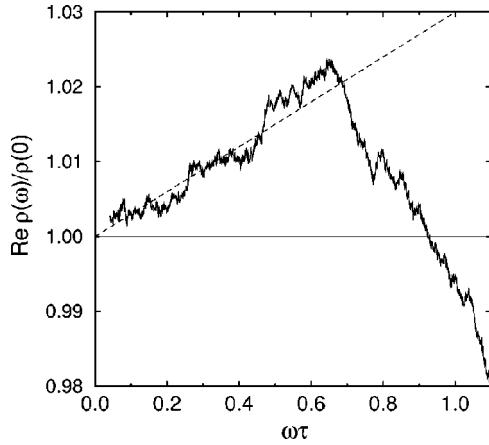


FIG. 5. Real part of the ac resistivity in the RMF, with $\alpha=0.5$ normalized to its $\omega=0$ value. The dashed line is a guide for the eye, $\Delta \text{Re } \rho(\omega)/\rho(0) \propto |\omega|$. The positive prefactor of the $|\omega|$ correction to $\text{Re } \rho$ corresponds to a negative prefactor for $\text{Re } \sigma$.

it is swamped by the statistical noise. A smaller value of the coefficient at $\alpha=0.5$ [as compared to the formula (44)] is further consistent with the fact that at $\alpha \geq 1$ the coefficient changes sign and the correction to the conductivity becomes positive (see below). Let us also note that the range of validity of the $|\omega|$ correction found numerically is in full agreement with the theoretical expectation ($\omega\tau \leq 1$). Indeed, as seen in Fig. 5, the linear increase of $\text{Re } \rho(\omega)$ holds up to $\omega\tau \approx 0.65$ where it transforms (rather abruptly) into a falloff (related to the ballistic motion on time scales $t \lesssim \tau$).

C. Strong random magnetic field: Long-time tail in transport on a percolating network

In a strong RMF ($\alpha \gg 1$) the character of the transport changes drastically. In this regime, diffusion takes place in a restricted space and is determined by a small fraction of trajectories—so-called “snake states”^{24,25}—which wind around the $B(\mathbf{r})=0$ contours. Since the snake states can go over from one $B(\mathbf{r})=0$ line to another at saddle points of the RMF (where the two contours come sufficiently close to each other), they propagate effectively on a percolating network^{26,14,15} for which such saddle points serve as nodes. This network is characterized¹⁵ by a typical length of a link, $L_s \sim d\alpha^{14/9}$, and a typical distance between two neighboring saddle points (size of an elementary cell), $\xi_s \sim d\alpha^{8/9}$. The different scaling of L_s and ξ_s with α is due to the fact that the structure of the links of the network is fractal. The network is chiral, i.e., the links are directed; each node has two incoming and two outgoing links. Since the snake-state velocity is of the order of the Fermi velocity, a characteristic time of traversal of a link is $\tau_s \sim L_s/v_F$. The quasiclassical dc conductivity in this regime was calculated in Refs. 14 and 15, the result being $\sigma \sim k_F d/\alpha^{1/2} \ln^{1/4} \alpha$.

In Ref. 15 we argued, on phenomenological grounds, that for such a percolation-type transport problem there should be a nonanalytic contribution to the ac conductivity of the form

$$\frac{\Delta \text{Re } \sigma(\omega)}{\sigma(0)} \sim |\omega| \tau_s, \quad |\omega| \tau_s \ll 1. \quad (45)$$

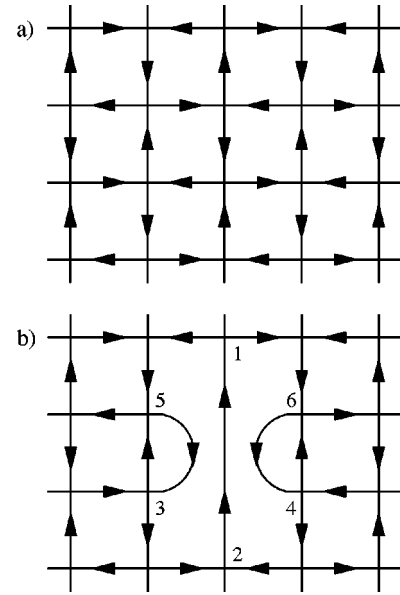


FIG. 6. Chiral network model: (a) Regular network; (b) defect on the lattice.

Below we demonstrate how this result comes about in a network model due to fluctuations in the geometry of the network.

Let us start with a regular square network [Fig. 6(a)] with all links characterized by the same distance ξ_s between the end points and by the same “flight time” τ_s . We also assume that the probability of turning in either of two allowed directions at each node is $1/2$. The classical diffusion constant is then $D = \xi_s^2/4\tau_s$. It is straightforward to see that there is no memory effect in classical transport on the regular network: the velocity correlation function is exactly zero for $t > \tau_s$. Let us now study the effect of fluctuations in the network geometry, i.e., in vectors connecting the beginning and end of individual links. Since to describe such fluctuations quantitatively in a real percolating network is hardly possible, we consider the following model. We imagine the regular lattice considered above perturbed by a small fraction $n_d \ll 1$ of “defects” of the type shown in Fig. 6(b) (a defect can have any of four possible directions). We assume the flight times of all links to be equal (we will discuss the effect of fluctuations in the flight times later).

For each lattice site j , we label adjacent links as $(j\mu)$, with $\mu=1$ and 2 for incoming links and $\mu=3$ and 4 for outgoing links. The velocity-velocity correlation function for a time $t=n\tau_s$ (with an integer n) can be written as

$$\langle \mathbf{v}(n\tau_s) \mathbf{v}(0) \rangle = \frac{1}{4N} \sum_{ij} \sum_{\mu=1,2} \sum_{\nu=3,4} \mathbf{v}_{i\mu} \mathbf{v}_{j\nu} P_{ij}[(n-1)\tau_s], \quad (46)$$

where N is the normalization factor (total number of sites), $P_{ij}(t)$ is the probability of moving from a site i to a site j in a time t , and $\mathbf{v}_{i\mu} = \xi_{i\mu}/\tau_s$ is the velocity at the link $(i\mu)$. The majority of the sites i and j will give zero contribution to Eq. (46) after the summation over μ and ν , since the velocities of the two outgoing (or two incoming) links are exactly opposite to each other for the regular lattice. A nontrivial contribution will come from terms with both i and j lying at a

defect. Indeed, consider the term with $i=1, j=2$ [Fig. 6(b)]. The corresponding contribution to Eq. (46) is

$$n_d P_{12}(t-\tau_s) \left(\frac{\xi_s}{\tau_s} \right)^2. \quad (47)$$

The probability density in a continuum model for a diffusing particle to move a distance \mathbf{r} in a time t is

$$P(t, \mathbf{r}) = \frac{1}{4\pi Dt} e^{-r^2/4Dt}. \quad (48)$$

Therefore, the probability $P_{12}(t)$ for $t \gg \tau_s$ is

$$P_{12}(t) = \frac{\tau_s}{\pi t} \left[1 + O\left(\frac{\tau_s}{t}\right) \right]. \quad (49)$$

This return process yields a contribution to the velocity correlation function of the form

$$n_d \left(\frac{\xi_s}{\tau_s} \right)^2 \frac{\tau_s}{\pi t} \propto \frac{1}{t}.$$

However, this $1/t$ contribution is canceled if we take into account the terms with $i=3$ and 4 and $j=5$ and 6 as well. The total contribution reads

$$\begin{aligned} \langle \mathbf{v}(t) \mathbf{v}(0) \rangle = & n_d \left(\frac{\xi_s}{\tau_s} \right)^{2f} \left[P_{12}(t-\tau_s) - P_{15}(t-\tau_s) - P_{32}(t-\tau_s) \right. \\ & \left. + \frac{1}{2} P_{35}(t-\tau_s) + \frac{1}{2} P_{36}(t-\tau_s) \right]. \end{aligned} \quad (50)$$

Since all of the relevant return probabilities P_{ij} have the form of Eq. (49), the $1/t$ terms cancel. It is easy to see that this cancellation has a general character, i.e., is independent of the particular structure of the defect. We thus conclude that the result is of the next order in τ_s/t :

$$\langle \mathbf{v}(t) \mathbf{v}(0) \rangle \sim -n_d \left(\frac{\xi_s}{\tau_s} \right)^2 \left(\frac{\tau_s}{t} \right)^2. \quad (51)$$

While we do not calculate the numerical coefficient in Eq. (51),²⁷ we see no reason which would require it to be zero, so that we believe that it is generically nonzero. Setting now $n_d \sim 1$ for a realistic (strongly fluctuating) network results in a nonanalytic correction to the conductivity of the form of Eq. (45). As to the sign of the effect, we have to resort to numerical simulations (see below).

Let us now consider the effect of fluctuations in flight time. We return to the regular square lattice (with the lattice constant ξ_s), but now allow for a variation of the flight times τ_μ from one link to another. We will show that in this model the $1/t^2$ tail does not exist. Equation (46) for the velocity-velocity correlation function is now modified as

$$\begin{aligned} \langle \mathbf{v}(t) \mathbf{v}(0) \rangle = & \frac{1}{4N\tau_s} \sum_{ij} \sum_{\mu=1,2} \sum_{\nu=3,4} \\ & \times \left\langle \int_0^{\tau_{i\mu}} d\tau \int_0^{\tau_{j\nu}} d\tau' \mathbf{v}_{i\mu} \mathbf{v}_{j\nu} P_{ij}(t-\tau-\tau') \right\rangle, \end{aligned} \quad (52)$$

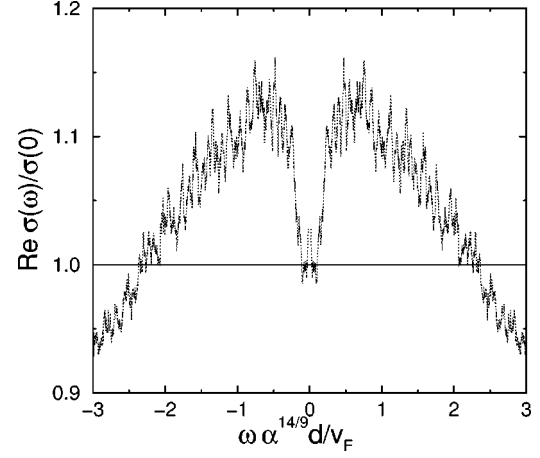


FIG. 7. Real part of the ac conductivity in the RMF at $\alpha = 4.04$. A nonanalytic dip around $\omega=0$ is clearly seen. The low-frequency increase of the conductivity is restricted to the region $|\omega|L_s/v_F \lesssim 1$ (where $L_s \sim d\alpha^{14/9}$ is the length of a link of the percolating network), in agreement with theory.

where $\mathbf{v}_{i\mu} = \xi_{i\mu}/\tau_\mu$ and $\tau_s = \langle \tau_\mu \rangle$. Since the fluctuations of the flight times of different links are uncorrelated, a nonzero contribution to Eq. (52) comes only from neighboring sites i and j connected by a link going from j to i [in other words, one of the links ($i\mu$) should be identical to one of the links ($j\nu$)]. We thus find

$$\begin{aligned} \langle \mathbf{v}(t) \mathbf{v}(0) \rangle = & \frac{1}{2} n_d \frac{\xi_s^2}{\tau_s} \left\langle \left\langle \int_0^{\tau_1} d\tau \int_0^{\tau_2} d\tau' \frac{1}{\tau_1 \tau_2} \right. \right. \\ & \times P_{ij}(t-\tau-\tau') \left. \left. \right\rangle_{\tau_1, \tau_2} \right. \\ & \left. - \left\langle \int_0^{\tau_1} d\tau \int_0^{\tau_1} d\tau' \frac{1}{\tau_1^2} P_{ij}(t-\tau-\tau') \right\rangle_{\tau_1} \right\rangle. \end{aligned} \quad (53)$$

Expanding $P_{ij}(t-\tau-\tau') \approx 1/\pi(t-\tau-\tau')$ in τ and τ' , we see that the terms of the $1/t$ and $1/t^2$ orders cancel, and the leading nonvanishing contribution is of the $1/t^3$ order, so that the corresponding contribution to $\text{Re } \sigma(\omega)$ shows a weak nonanalyticity $\propto \omega^2 \ln|\omega|$ only. Note that for a nondirected network, fluctuations of the flight time yield a still weaker nonanalyticity $\Delta \text{Re } \sigma(\omega) \propto |\omega|^3$, or, equivalently, a $1/t^4$ long-time tail.²⁸

Since a real percolating network exhibits all possible sorts of fluctuations, the fact that we find the $1/t^2$ tail in the model with fluctuating ξ_μ 's is sufficient to conclude that such a tail should be present in the problem of the transport in strong RMF. In Fig. 7 we show the results of the numerical simulations of the problem for $\alpha \approx 4$. A pronounced dip in the ac conductivity around $\omega=0$ in the expected range of frequencies $|\omega| \lesssim 1/\tau_s \sim v_F/d\alpha^{14/9}$ nicely confirms our analytical conclusions. The sign of the nonanalytic correction corresponds to a decrease of $\text{Re } \sigma$ as $|\omega| \rightarrow 0$.

It is worth mentioning that the problem of a random walk on such a percolating network is a close relative of the advection-diffusion problem in a spatially random velocity

field $\mathbf{v}(\mathbf{r})$ (“steady flow”) with $\nabla \cdot \mathbf{v} = 0$ (“incompressible liquid”) characterized by the correlation function

$$\int d^2r \exp(-i\mathbf{q}\mathbf{r}) \langle v_\alpha(0)v_\beta(\mathbf{r}) \rangle = \tilde{W}_v(q) (\delta_{\alpha\beta}q^2 - q_\alpha q_\beta). \quad (54)$$

This model was studied in a series of papers,^{29–31} with an emphasis on the case of long-range correlations, namely, $\tilde{W}_v(q) \propto q^{-2}$ for $q \rightarrow 0$ [which corresponds to $\langle v_\alpha(0)v_\beta(\mathbf{r}) \rangle \propto r^{-2}$]. In contrast, we have considered a percolation lattice with short-scale distortions [$\tilde{W}_v(q) \rightarrow \text{const}$ at $q \rightarrow 0$]. One can check (see the Appendix) that the advection-diffusion problem yields a t^{-2} tail in this case, in agreement with our consideration above.

IV. EFFECT OF INELASTIC SCATTERING

So far our considerations have not included inelastic scattering processes which change the energy of a particle. The question arises whether the zero-frequency anomaly $\Delta \text{Re } \sigma(\omega)$ is cut off at low frequencies $\omega \sim 1/\tau_{\text{in}}$, where τ_{in} is a relaxation time for the inelastic processes. This question is studied most conveniently within the Liouville-Boltzmann approach of Sec. III. To this end, we consider the linearized distribution function $\delta f(\omega, \mathbf{r}, \epsilon, \phi)$ of particles with energy ϵ and velocity direction specified by the polar angle ϕ , subject to a smooth RP or RMF and inelastic collision processes, obeying the Liouville-Boltzmann equation

$$(-i\omega + \mathbf{v}\nabla + \delta L)\delta f - I_{\text{in}}(\delta f) = S, \quad (55)$$

with the source term $S = e\mathbf{v}\mathbf{E}(\partial f_0/\partial \epsilon)$. Here f_0 is the Fermi distribution function corresponding to a temperature T (which we will assume to be low, $T \ll E_F$). A simple model form of the collision integral I_{in} , which respects particle number conservation, is sufficient for our purposes:

$$I_{\text{in}}(\delta f) = -\frac{1}{\tau_{\text{in}}} \left[\delta f(\epsilon, \phi) + \frac{\partial f_0}{\partial \epsilon} \int d\epsilon' \int \frac{d\phi'}{2\pi} \delta f(\epsilon', \phi') \right]. \quad (56)$$

(For simplicity we adopt the model of isotropic, energy independent inelastic scattering.)

The conductivity is obtained as

$$\sigma(\omega) = e^2 v v_F^2 \int d\epsilon \left(-\frac{\partial f_0}{\partial \epsilon} \right) \int \frac{d\phi}{2\pi} \left\langle \cos \phi \frac{1}{\tilde{L}_0} \cos \phi \right\rangle, \quad (57)$$

where $\tilde{L}_0 = -i\omega + \tau_{\text{in}}^{-1} + v_F \mathbf{n}\nabla$. Expanding in δL , averaging over the long-range disorder and resumming the series, one finds $\sigma(\omega)$ in the form of Eq. (27). The memory function M is now given in lowest order for the cases of RP and RMF by Eqs. (30) and (41), respectively, with ω replaced by $\omega + \tau_{\text{in}}^{-1}$.

In order to calculate the effect of return processes, one needs to know the diffusion propagator $\tilde{P}_D(\mathbf{q}; \epsilon, \phi; \epsilon', \phi')$ for particles starting with energy ϵ and velocity angle ϕ and returning with energy ϵ' and angle ϕ' . This obeys Eq. (55) with the source term replaced by $S_D = \delta(\phi - \phi')\delta(\epsilon - \epsilon')(-\partial f_0/\partial \epsilon)$. After averaging over δL , one finds

$$\tilde{P}_D(\mathbf{q}; \epsilon, \phi; \epsilon', \phi') = \left(\frac{\partial f_0}{\partial \epsilon} \right) \frac{\gamma_\epsilon(\mathbf{q}, \phi) \gamma_{\epsilon'}(\mathbf{q}, \phi')}{D_t q^2 - i\omega} \left(\frac{\partial f_0}{\partial \epsilon'} \right) + (\text{regular terms}), \quad (58)$$

where $D_t = v_F^2 \tau_t / 2$ with $\tau_t^{-1} = \tau^{-1} + \tau_{\text{in}}^{-1}$ is the total diffusion constant including elastic and inelastic scattering processes, and $\gamma_\epsilon(\mathbf{q}, \phi) = [1 - iqv(\epsilon)\tau_t \cos(\phi - \phi_q)]$, with $v(\epsilon) = (2\epsilon/m)^{1/2}$. As expected, the diffusion propagator shows a diffusion pole even in the presence of inelastic processes, due to particle number conservation. The scattering “out” of particles with given energy ϵ into other energy states is exactly compensated for by a corresponding scattering-in contribution.

Let us define the function $\Delta M(\epsilon, \epsilon')$ in the same way as in Eqs. (35) and (42), with the only change $P_D(\mathbf{q}, \phi, \phi') \rightarrow \tilde{P}_D(\mathbf{q}; \epsilon, \phi; \epsilon', \phi')$. The correction to the memory function due to return processes, ΔM , is then given by

$$\Delta M = \int d\epsilon d\epsilon' \Delta M(\epsilon, \epsilon'). \quad (59)$$

As a result, expressions (37) and (39) and (43) and (44) remain valid, provided (i) τ and l are replaced by the full momentum relaxation time τ_t and mean free path $l_t = v_F \tau_t$, respectively; and (ii) additional factors of $(\tau_t/\tau)^2$ and τ_t/τ are included in Eqs. (39) and (44), respectively, which stem from the explicit factors of \tilde{W} in the definition of $\Delta M(\epsilon, \epsilon')$.

Thus the classical zero-frequency anomaly is not cut off at finite temperature. This should be contrasted with the quantum zero-frequency anomaly induced by the weak-localization and Altshuler-Aronov (interplay of interaction and disorder) effects. It follows that increasing temperature favors the experimental observation of the classical anomaly.

V. CONCLUSIONS

In this paper, we have studied memory effects in the low-frequency ac conductivity of a 2D fermion gas in a long-range random potential or random magnetic field. We have calculated the long-time tail in the velocity correlation function induced by diffusive returns of a particle, and leading to a nonanalytic $|\omega|$ behavior of the real part of the conductivity (zero-frequency anomaly). While in a random potential the $|\omega|$ contribution is positive (as in the Lorentz gas, Ref. 1) and is proportional to $(d/l)^2$, where $d/l \ll 1$ is the ratio of the correlation length to the mean free path, a smooth weak RMF induces a much larger ($\propto d/l$) correction of opposite sign. The sign difference can be traced back to the RMF scattering being odd with respect to time reversal.

We have also demonstrated how an $|\omega|$ contribution to $\text{Re } \sigma(\omega)$ arises in the regime of strong random magnetic field, where the transport is determined by percolation of the snake states. In this case, spatial fluctuations in the geometry of the percolating network are responsible for the memory effects.

Our numerical simulations confirm the existence of these nonanalytic contributions at low frequency, as well as the unconventional sign of the correction in the weak random magnetic field. With increasing strength of the RMF, when the system crosses over into the regime of the percolating

transport, the sign of the effect changes.

The experimental observation of the nonanalytic low-frequency behavior of the ac conductivity of composite fermions would be of considerable interest. In particular, we predict that the $|\omega|$ term in $\text{Re } \sigma$ is negative at $\nu=1/2$ in the high-mobility samples (where the strength of the effective RMF is¹⁵ $\alpha \sim 0.3$), but should change sign if the system is driven toward the percolation regime by adding more long-range scatterers (e.g., antidots³²). A sign change is also found with increasing effective magnetic field (moving away from half-filling), as will be demonstrated analytically elsewhere,³³ in agreement with our earlier numerical results.¹⁵

ACKNOWLEDGMENTS

We are grateful to D. Khmelnitskii for discussions of the role of inelastic scattering and to Y. Levinson for attracting our attention to Ref. 17. This work was supported by SFB 195 and the Schwerpunktprogramm ‘‘Quanten-Hall-Systeme’’ of the Deutsche Forschungsgemeinschaft, by INTAS Grant No. 97-1342, and by the German-Israeli Foundation.

APPENDIX

Consider a particle moving in a diffusive medium with a diffusion coefficient D , subject to a spatially random velocity field $\mathbf{v}(\mathbf{r})$. Let the velocity field be incompressible ($\nabla \cdot \mathbf{v} = 0$) and determined by correlator (54) with a finite $\tilde{W}_v(0)$.

Assuming the random field to be weak, we can expand the Green’s function

$$G(\mathbf{r}, \mathbf{r}') = \langle \mathbf{r} | (-i\omega - D\nabla^2 - \nabla \cdot \mathbf{v})^{-1} | \mathbf{r}' \rangle$$

in $\mathbf{v}(\mathbf{r})$, which yields, for the Fourier transform,

$$\begin{aligned} \tilde{G}(q) &\simeq \frac{1}{-i\omega + Dq^2} \\ &+ \frac{1}{(-i\omega + Dq^2)^2} \left\langle (\mathbf{v} \cdot \nabla) \frac{1}{-i\omega - D\nabla^2} (\mathbf{v} \cdot \nabla) \right\rangle_q \\ &+ \dots \end{aligned}$$

Using the correlation function (54) and resumming the series, we thus find

$$\tilde{G}(q) = \frac{1}{-i\omega + (D + \delta D)q^2},$$

with the following correction to the diffusion coefficient:

$$\delta D = \frac{3}{2} \int \frac{d^2q}{(2\pi)^2} \frac{q^2 \tilde{W}_v(q)}{-i\omega + Dq^2} \simeq -\frac{3}{16} \frac{\tilde{W}_v(0)}{D^2} |\omega|.$$

Hence this continuous model predicts a t^{-2} tail in the velocity-velocity correlation function, with a positive coefficient. Note, however, that in a lattice model the sign depends on the microscopic structure of disorder.

*Also at Petersburg Nuclear Physics Institute, 188350 St. Petersburg, Russia.

†Also at A. F. Ioffe Physico-Technical Institute, 194021 St. Petersburg, Russia.

¹M. H. Ernst and A. Weyland, Phys. Lett. **34A**, 39 (1971).

²E. H. Hauge, in *Transport Phenomena*, edited by G. Kirczenov and J. Marro, Lecture Notes in Physics Vol. 31 (Springer, Berlin, 1974), p. 337.

³C. P. Lowe and A. J. Masters, Physica A **195**, 149 (1993); A. Kuzmany and H. Spohn, Phys. Rev. E **57**, 5544 (1998).

⁴A simple qualitative explanation of the tail [Eq. (4)] is as follows.

In the Lorentz gas model, a particle starting at an arbitrary point at $t=0$ in the x direction moves freely during a time $\sim l/v_F$, until it reaches the first scatterer, after which it starts to diffuse. The long-time tail arises due to the memory of the fact that between $t=0$ and the first scattering no scatterers have been hit, i.e., that the corresponding rectangle with an area $\sim al$ is free of scatterers. The probability of return to this area is $\sim al/Dt$. Now, returning particles will have, on average, a negative projection of $v_x \sim -l/t$. Due to the memory effect specified above, these particles will not be scattered, thus giving a negative tail $\langle v_x(t)v_x(0) \rangle \sim -v_F(al/Dt)(l/t) \sim -al/t^2$, in agreement with Eq. (4). For the Lorentz gas, the condition for the classical derivation to be valid is $k_F a^2 \gg l$, where k_F is the Fermi wave vector.

⁵See, e.g., P. A. Lee and T. V. Ramakrishnan, Rev. Mod. Phys. **57**, 287 (1985).

⁶B. I. Halperin, P. A. Lee, and N. Read, Phys. Rev. B **47**, 7312 (1993).

⁷S. J. Bending, K. von Klitzing, and K. Ploog, Phys. Rev. Lett. **65**, 1060 (1990).

⁸A. Geim, S. Bending, and I. Grigorieva, Phys. Rev. Lett. **69**, 2252 (1992); A. Geim, S. Bending, I. Grigorieva, and M. G. Blamire, Phys. Rev. B **49**, 5749 (1994).

⁹F. B. Mancoff, R. M. Clarke, C. M. Marcus, S. C. Zhang, K. Campman, and A. C. Gossard, Phys. Rev. B **51**, 13 269 (1995); L. Zielinski, K. Chaltikian, K. Birnbaum, C. M. Marcus, K. Campman, and A. C. Gossard, Europhys. Lett. **42**, 73 (1998).

¹⁰P. D. Ye, D. Weiss, G. Lütjering, R. R. Gerhardt, K. von Klitzing, K. Eberl, H. Nickel, and G. Weimann, in *Proceedings of the 23rd International Conference on The Physics of Semiconductors* (World Scientific, Singapore, 1996), p. 1529.

¹¹A. W. Rushforth, B. L. Gallagher, P. C. Main, A. C. Neumann, C. H. Marrows, I. Zoller, M. A. Howson, B. J. Hickey, and M. Henini, contribution to EP2DS-13 (Ottawa, 1999).

¹²G. M. Gusev, J. R. Leite, A. A. Bykov, N. T. Moshegov, V. M. Kudryashev, A. I. Toropov, and Yu. V. Nastaushv, Phys. Rev. B **59**, 5711 (1999).

¹³D. V. Khveshchenko, Phys. Rev. Lett. **77**, 1817 (1996).

¹⁴A. D. Mirlin, D. G. Polyakov, and P. Wölfle, Phys. Rev. Lett. **80**, 2429 (1998).

¹⁵F. Evers, A. D. Mirlin, D. G. Polyakov, and P. Wölfle, Phys. Rev. B **60**, 8951 (1999).

¹⁶S. V. Maleev and B. P. Toperverg, Zh. Éksp. Teor. Fiz. **69**, 1440 (1975) [Sov. Phys. JETP **42**, 734 (1976)].

¹⁷S. V. Gantsevich, V. D. Kagan, and R. Katilyus, Zh. Éksp. Teor. Fiz. **80**, 1827 (1981) [Sov. Phys. JETP **53**, 946 (1981)].

¹⁸D. Belitz, A. Gold, and W. Götzke, Z. Phys. B: Condens. Matter **44**, 273 (1981).

¹⁹A. D. Mirlin, E. Altshuler, and P. Wölfle, Ann. Phys. (Leipzig) **5**, 281 (1996).

- ²⁰The fact that $S_x(\mathbf{q}) \propto q$ ensures the absence of divergent (at $\omega = 0$) one-diffuson contributions to $\Delta\sigma(\omega)$ of the type $\int d^2q/(Dq^2 - i\omega)$; see D. Vollhardt and P. Wölfle, Phys. Rev. B **22**, 4666 (1980).
- ²¹A. D. Mirlin, J. Wilke, F. Evers, D. G. Polyakov, and P. Wölfle, Phys. Rev. Lett. **83**, 2801 (1999).
- ²²It is instructive to plot the memory function (rather than the conductivity), since it would be constant in the Drude approximation [while $\text{Re } \sigma(\omega)$ has a Lorentzian shape]. In the weak-disorder regime, deviations from the Drude approximation are relatively weak, and are much better seen in $\text{Re } \rho(\omega)$ than in $\text{Re } \sigma(\omega)$.
- ²³In a related calculation of the magnetoresistivity (Ref. 21) we found that the analytical result for small α is in quantitative agreement with the numerical simulations for $\alpha \leq 0.01$, while it correctly describes qualitative features up to $\alpha \sim 0.5$.
- ²⁴J. E. Müller, Phys. Rev. Lett. **68**, 385 (1992).
- ²⁵D. B. Chklovskii and P. A. Lee, Phys. Rev. B **48**, 18 060 (1993).
- ²⁶D. K. K. Lee, J. T. Chalker, and D. Y. K. Ko, Phys. Rev. B **50**, 5272 (1994).
- ²⁷The continuum approximation [Eq. (48)] is not sufficient to find the numerical prefactor of the correction term in Eq. (49), i.e., of the contributions $\sim (\tau_s/t)^2$ to $P_{ij}(t)$.
- ²⁸J. Wilke, Diploma thesis, Karlsruhe, 1999.
- ²⁹B. Derrida and J. M. Luck, Phys. Rev. B **28**, 7183 (1983).
- ³⁰D. S. Fisher, Phys. Rev. A **30**, 960 (1984); D. S. Fisher, D. Friedan, Z. Qiu, S. J. Shenker, and S. H. Shenker, *ibid.* **31**, 3841 (1985).
- ³¹V. E. Kravtsov, I. V. Lerner, and V. I. Yudson, Zh. Éksp. Teor. Fiz. **91**, 569 (1986) [Sov. Phys. JETP **64**, 336 (1986)].
- ³²J. H. Smet, D. Weiss, K. von Klitzing, P. T. Coleridge, Z. W. Wasilewski, R. Bergman, H. Schweizer, and A. Scherer, Phys. Rev. B **56**, 3598 (1997).
- ³³F. Evers, A. D. Mirlin, D. G. Polyakov, and P. Wölfle (unpublished).